Available online at www.sciencedirect.com
SCIENCE DIRECT®
Journal of Chromatography A, 1068 (2005) 107–114
JOURNAL OF CHROMATOGRAPHY A
www.elsevier.com/locate/chroma

Effect of initial voltage ramp on separation efficiency in non-aqueous capillary electrophoresis with ethanol as background electrolyte solvent

Sami Palonen*, Matti Jussila, Marja-Liisa Riekkola

Laboratory of Analytical Chemistry, Department of Chemistry, P.O. Box 55, FI-00014 University of Helsinki, Helsinki, Finland

Abstract

Band broadening at high electric field strengths in capillary electrophoresis (CE), especially in wide capillaries, is often attributed to radial temperature gradients in the interior of the capillary caused by Joule heating. In some cases, however, a major cause of the lower separation efficiency could be the abrupt application of high electric field strength. We show that, with ethanol as background electrolyte solvent, initial abrupt voltage application introduces band broadening, which is especially pronounced in wider capillaries at high electric field and ionic strengths. With an appropriate initial voltage ramp this effect can be avoided. The effect of different voltage ramp up times on the separation efficiency of some anionic analytes was investigated with 50, 75 and 100 μm I.D. capillaries at field strengths of 1000–2000 V cm^{-1}. The results suggest that the band broadening associated with abrupt voltage application is of thermal origin and probably related to thermal volume expansion of the sample and background electrolyte solutions. The plate numbers calculated with a plate height model were in good agreement with the experimental values when a sufficiently long voltage ramp was employed. The dispersion due to axial temperature gradients was found to be very small under the experimental conditions used.

Keywords: Voltage ramp; Capillary electrophoresis; Separation efficiency; Dispersion; Axial temperature gradient; Joule heating

1. Introduction

Temperature affects nearly all parameters involved in capillary electrophoresis (CE). The fluid-filled separation capillary inevitably heats up due to the friction assosiated with the movement of ionic species during the separation. As a check on this, most CE instruments have active temperature control systems. Joule heating [1–3] generates a radial temperature gradient, which is the best-known thermal dispersive effect. It has nevertheless been shown [2–6] that, under most conditions, radial temperature gradients are a fairly insignificant source of dispersion in CE. Radial temperature gradients (often referred to as Joule heating when band broadening is discussed) are thus sometimes blamed for low efficiencies though the cause of the dispersion lies elsewhere. Axial variations in the electroosmotic flow (EOF) [7–11] are another source of dispersion. These occur when EOF velocities vary in the different regions of the capillary setting up a pressure gradient, which will introduce additional dispersion due to the unfavorable flow profile of hydrodynamic flow. Axial variations in EOF velocities are caused by variations in zeta potential along the capillary, for example, due to only partial coating of the capillary [8] or to partial capillary exposure to an external radial electric field [9]. Another source of axial variations in EOF is variations in viscosity due to axial temperature differences in the capillary [12–14]. Typically in a modern CE instrument, the middle region of the capillary is well thermostatted, whereas the inlet and outlet regions lack temperature control. Relatively strong axial variations in temperature are thus common in CE. It should be added that, in most cases, the unthermostatted inlet and outlet regions represent large percentages of the total length of the capillary.

Recently, Xuang and Li [12] derived an analytical equation for the part of the plate height that is due to both axial and radial temperature gradients (H_T):

$$H_T = \frac{r_c^2}{24 L_{det}} \sum_{i=1}^{3} \frac{v_{i,pd}^2 t_i}{D_i} \quad (1)$$

* Corresponding author. Fax: +358 9 19150253.
E-mail address: sami.palonen@helsinki.fi (S. Palonen).

0021-9673/$ – see front matter © 2005 Elsevier B.V. All rights reserved.
doi:10.1016/j.chroma.2005.01.064

Here r_c is the internal radius of the capillary and L_{det} is the capillary length to the detector. The subscript i represents the different regions of the capillary: (1) is for the inlet unthermostatted region, (2) is for the middle thermostatted region and (3) is for the outlet unthermostatted region. $v_{i,pd}$ is the velocity contributing to the band broadening and D_i and t_i represent the average diffusion coefficient and residence time in region i, respectively. In the case of charged analytes $v_{i,pd}$ consists of two contributions that are coupled, namely the pressure induced velocity due to the axial temperature gradients and the velocity related to the electrophoretic mass flow distortion due to the radial temperature gradient:

$$v_{i,pd} = \frac{-M_i \Delta P_i}{L_i} + \frac{1}{2}\omega_i \mu_{i,ep} E_i \quad (2)$$

where M_i, ΔP_i, $\mu_{i,ep}$ and E_i represent the "hydrodynamic conductivity" (see below), pressure difference and electrophoretic mobility of the analyte and the electric field strength in region i, respectively [12]. L_i is the length of region i and

$$\omega_i = B\frac{\Delta T_{ic}}{T_{iw}^2} \quad (3)$$

where B is a constant representing the exponential temperature dependency of viscosity and ΔT_{ic} is the difference between the temperature of the capillary inner wall (T_{iw}) and temperature at the centre of the capillary in region i. M_i in Eq. (2) can be expressed as:

$$M_i = \left(1 + \frac{1}{3}\omega_i\right)\frac{r_c^2}{8\eta_{iw}} \quad (4)$$

where η_{iw} is the viscosity of the solution near the capillary wall in region i [12]. Pressure differences are obtained by calculating the EOF induced pressures at the interfaces of the thermostatted and unthermostatted regions [12]:

$$P_1 = \frac{\mu_{2,eo}E_2 - \mu_{1,eo}E_1}{\frac{M_1}{L_1} + \frac{M_2}{L_2}\left(1 + \frac{L_3}{L_1}\right)} \quad (5)$$

$$P_2 = -P_1\frac{L_3}{L_1} \quad (6)$$

where $\mu_{i,eo}$ is the velocity of the EOF at T_{iw}. The electric field strengths in the different regions can be calculated from the current continuity condition $\kappa_1 E_1 = \kappa_2 E_2 = \kappa_3 E_3$, where κ_i is the electrical conductivity of the background electrolyte (BGE) solution ($\kappa_1 > \kappa_2$ because $T_{1,iw} > T_{2,iw}$). Note that for neutral analytes $\mu_{i,ep} = 0$ and thus H_T is affected only by axial temperature gradients (Eqs. (1) and (2)). For more details, see Ref. [12].

Knox and McCormack [15] have suggested that sample loss can occur in CE due to the initial self-heating and resulting volume expansion. As a precaution they recommend that the rate of increase of voltage during switch-on should be below a critical (maximum) value dU/dt:

$$\frac{dU}{dt} < \frac{\frac{\mu_{tot}R_\Omega}{\gamma\alpha_{PT}}}{1 + \delta\Delta T_{inlet}} \quad (7)$$

where U is voltage and t time, μ_{tot} is the total mobility of the last migrating analyte ion and R_Ω is the resistance per unit length of the capillary filled with BGE solution. γ, α_{PT}, and δ represent the coefficient of expansion of the BGE solution, the power–temperature coefficient and the temperature coefficient of viscosity, respectively. ΔT_{inlet} is the capillary core temperature increase relative to the temperature of the surroundings at the inlet side of the capillary, which can be expressed as:

$$\Delta T_{inlet} = \frac{EI}{2\pi}\left(\frac{1}{2k_b} + \frac{1}{k_s}\ln\frac{r_w}{r_c} + \frac{1}{k_p}\ln\frac{r_p}{r_w} + \frac{1}{h_1 r_p}\right) \quad (8)$$

where EI is the heating power per unit length obtained directly from E and the measured current (I) in the capillary and k_b, k_s and k_p are the thermal conductivities of the BGE solution, the fused silica wall and the outer polymer coating [4]. r_w and r_p are the external radius of the silica tube and the external radius of the whole capillary (outer polymer coating included), respectively, while h_1 is the surface heat transfer coefficient at the inlet of the capillary. Note that the value of h_1 tends to be rather low because the inlet part of the capillary is not thermostatted and heat dissipation is governed mainly by free convection to still air, which results to elevated temperatures [16].

This study is a continuation of our previous work on separation efficiencies at high field strengths in non-aqueous CE [17–19]. Most recently [19], we found that the observed separation efficiencies (measured as plate numbers) of anionic model analytes in 75 μm I.D. capillaries at 60 kV were considerably lower that the values predicted by an analytical plate height model. With lower field strengths and narrower capillaries, however, agreement between the observed and predicted values was fairly good. The prediction showed that the contribution of Joule heating (via radial temperature gradients) to total plate height was insignificant (<5%) in all cases, but the increase of dispersion with E and r_c indicated that the dispersion could be of thermal origin. In this study we attempt to clarify the reasons for the deviation between predicted and experimental values at higher field strengths in 75 μm I.D. capillaries.

2. Materials and methods

2.1. Chemicals, BGEs and sample solutions

All chemicals were used as received and were of analytical-reagent grade unless otherwise stated. 2,6-dichlorobenzoic acid and 2,4-dinitrobenzoic acid were from Aldrich (Milwaukee, WI, USA). 3,5-Dinitrobenzoic acid was from Fluka (Buchs, Switzerland) and 2,4-dinitrophenol was

from Eastman Organic Chemicals (Rochester, NY, USA). Ethanol (EtOH) was from Primalco (Rajamäki, Finland) and HPLC-grade methanol (MeOH) was from J.T. Baker (Deventer, The Netherlands).

Equimolar amounts of sodium acetate (NaAc, from E. Merck, Darmstadt, Germany) and acetic acid (HAc, from Riedel-de Haën, Seelze, Germany) were added to EtOH to achieve a buffered BGE. Sample solution consisting of benzoic acids and a phenolic compound was prepared in MeOH (10 μg/mL each).

2.2. CE instrument and related parameters

The CE instrument was a laboratory-constructed model [20] capable of performing separations with 60 kV potential differences (for details, see Refs. [17–20]). Negative polarity was used throughout the study. The capillaries were of fused silica (Composite Metal Services, Hallow, United Kingdom) with I.Ds. of 50, 75 or 100 μm. O.D. of the capillaries was always 375 μm and the total length was 30 cm, while length to the detector window was 28.5 cm. As in our previous work [19], to suppress the EOF poly(glycidylmethacrylate-co-*N*-vinylpyrrolidone) [poly(GMA-co-NVP)] coating was applied to all capillaries. Injections were performed by siphoning with a 20 mm level difference for 45, 20 and 12 s for the 50, 75, and 100 μm I.D. capillaries, respectively. Analytes were detected at 214 nm. Capillary thermostatting was done with air flow cooling at 23 °C and the electric current ranged from 5 to 51 μA.

3. Results and discussion

In an attempt to discover the cause of lowered separation efficiencies in 75 μm I.D. capillaries with 15 mM acetate BGE at high field strengths, we conducted investigations with the same BGE solution and model compounds as previously [19]. The results obtained with various voltage ramps and capillaries of different I.D. are considered first, and then the effect of ionic strength of the BGE solution on the band broadening is discussed. Finally, heating powers and critical dU/dt values, as well as plate height increase due to the combined effect of axial and radial temperature gradients, are calculated and discussed in relation to the observed dispersion trends.

3.1. Effect of initial voltage ramp

We suspected at the time of our earlier work that the thermal conditions at the unthermostatted inlet of the capillary were causing some dispersion of the analyte zones. In view of this, we decided to apply somewhat lower voltages at first and then to increase the separation potential with various voltage ramps. Linear ramps were used throughout the study. The measured separation efficiencies, or peak widths, are compared with those obtained with no initial ramp.

3.1.1. Initial voltage ramp and time addition compensation

The initial voltage ramp had a pronounced effect on the separation efficiency with 75 μm I.D. capillaries at 60 kV. The plate numbers were only about 90,000 when no initial voltage ramp was used but increased more or less linearly with increasing initial ramp time (t_{ramp}) up to about 300,000 at t_{ramp} = 45 s. These plate numbers calculated from the measured migration time and peak width are, however, not directly comparable with our previous results [19] since the electric field strength was not constant during the run and thus the migration times were affected. Likewise, the results obtained with the different ramps cannot easily be compared to each other. For example, relative to the no ramp condition, an initial voltage ramp time of 30 s resulted in 25% increase in the migration time of the fastest analyte (2,4-dinitrophenol) at 60 kV, which in turn led to overestimated separation efficiencies in plate number calculation. Fortunately, this problem can be avoided by focusing on the peak widths (Fig. 1A). As can be seen from Fig. 1A, an introduction of a voltage ramp indeed provides narrower peaks. To allow better comparison with our previous results [19], we calculated "corrected plate numbers", N_{corr}, with the following equation:

$$N_{corr} = 16\left(\frac{t_{migr,no\ ramp}}{w_{b,ramp}}\right)^2 \quad (9)$$

where $t_{migr,no\ ramp}$ is the average migration time of the analyte in the case of no initial voltage ramp and $w_{b,ramp}$ is the peak width of the analyte at the baseline level with an initial voltage ramp. "Correcting" in our case thus means that when calculating plate numbers we always use the average migration time of the analyte with no initial ramp, but insert the peak width obtained with a specific initial ramp. Our approach is similar to that of Williams and Vigh [21], who corrected migration times in the calculation of analyte mobilities. Migration times were prolonged due to the initial linear voltage ramp, but they achieved the correction mathematically simply by subtracting a factor of $0.5 \times t_{ramp}$ from the measured migration time. Unlike them, however, we have access to true average migration times without the ramp. Eq. (9) has the disadvantage that the peak width that is used includes contributions from all time-dependent dispersion effects, like the diffusion, that occur during the extra time (e.g. 20 s), that the analyte spends in the capillary due to the voltage ramp. Migration time in Eq. (9) does not include that extra time. The corrected efficiency calculated from Eq. (9), however, gives a reasonable low-end approximation for the separation efficiency. The calculated corrected plate numbers are presented in Fig. 1B and, as can be seen, the ramp clearly improves the efficiencies. There seems to be a maximum in the efficiency with initial voltage ramp time of about 30 s, but good efficiencies are achieved even with a 15 s ramp.

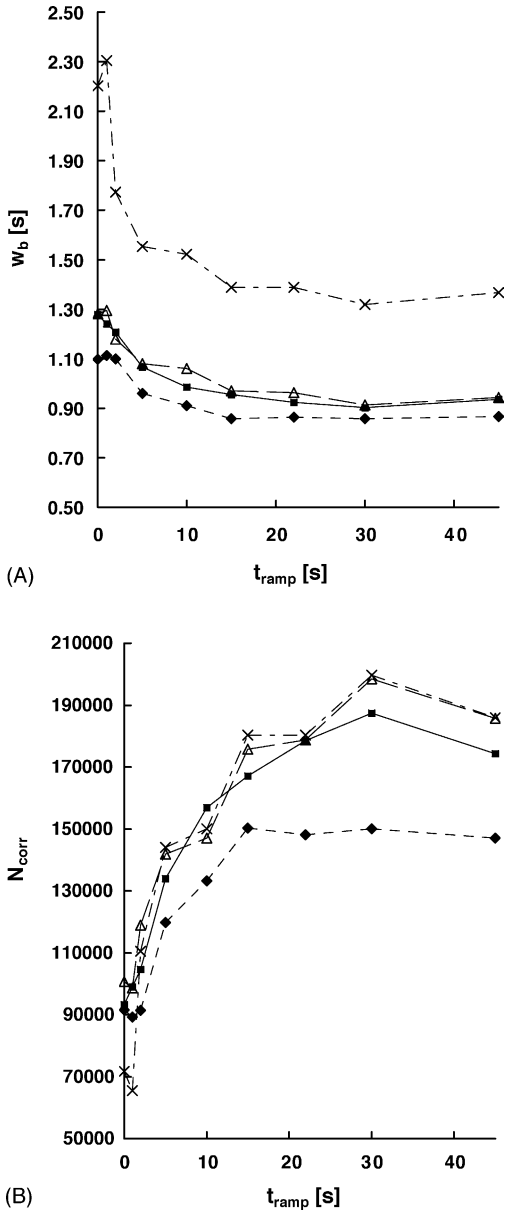

Fig. 1. Dependence of (A) peak width and (B) corrected plate number on the initial voltage ramp up time (t_{ramp}) with 75 μm I.D. poly(GMA-co-NVP) coated capillaries at 60 kV (2000 V cm^{-1}). BGE: 15 mM NaAc + 15 mM HAc in EtOH. Capillary, 30 cm total length, 28.5 cm to detector; detection, UV 214 nm; hydrodynamic injection, 20 mm for 20 s; analyte concentration, 10 μg/ml each; air flow thermostatting, 23 °C; number of repetitions, 6. Symbols: (♦) 2,4-dinitrophenol; (■) 3,5-dinitrobenzoic acid; (Δ) 2,4-dinitrobenzoic acid; (×) 2,6-dichlorobenzoic acid.

3.1.2. Initial voltage ramp and final separation voltage

The initial voltage ramp had only a little effect on the corrected plate numbers at 30 kV separation voltage (1000 V cm^{-1}) and in contrast to the results obtained at 60 kV, the corrected plate numbers tended to slightly decrease with increasing ramp time (approximately from 190,000 at t_{ramp} = 0 s to 170,000 at t_{ramp} = 45 s). This suggests that the use of initial voltage ramp is not beneficial at lower field strengths and that the dispersive effect associated with initial abrupt voltage application is dependent on the final separation voltage.

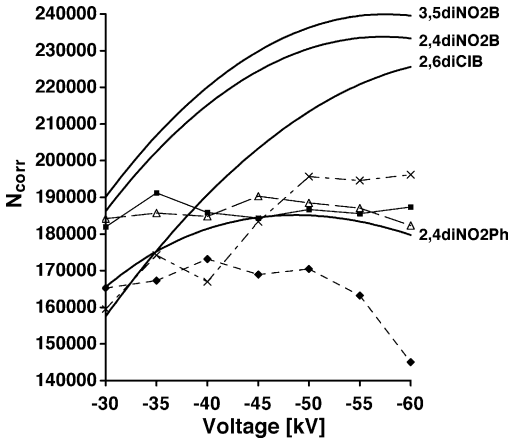

Fig. 2. Corrected plate numbers (symbols) obtained experimentally using 75 μm I.D. coated capillary with 30 s initial voltage ramp and calculated plate numbers (solid lines) obtained using the plate height model [18,19] at various separation voltages. Abbreviations: 2,4diNO2Ph, 2,4-dinitrophenol; 3,5diNO2B, 3,5-dinitrobenzoic acid; 2,4diNO2B, 2,4-dinitrobenzoic acid; 2,6diClB, 2,6-dichlorobenzoic acid. For other parameters, see Fig. 1.

3.1.3. Comparison with theory: 30 s initial voltage ramp with 75 μm I.D. capillaries

Since 30 s initial voltage ramp was found be beneficial at 60 kV, this was selected as ramp time in all following experiments. Fig. 2 shows the effect of separation voltage on N_{corr} with the 30 s ramp time, as well as the calculated values obtained earlier [19] from the plate height model. The values agree fairly well, though the experimental values are still somewhat lower than the values calculated with the model. Note, however, that the average RSD of the corrected separation efficiencies was about 9% and that the corrected efficiencies should be viewed as low-end approximations (see Eq. (9) and the discussion on corrected plate numbers). The severe broadening observed in our previous work (N only about 50,000–90,000 at 60 kV [19]), was not evident in the new experiments with 30 s initial voltage ramp and thus we conclude that the additional broadening observed previously was mainly due to the initial abrupt voltage application.

3.1.4. Initial voltage ramp and capillary diameter

Fig. 3 compares the experimental N_{corr} values obtained using a 30 s ramp time and 50 μm I.D. capillary with efficiencies obtained from the plate height model [19]. The agreement of the predicted and observed values is generally very good. Comparison with our earlier findings [19] under the same experimental conditions but without the initial voltage ramp reveals that the values with and without the ramp are close to each other (data not shown). Thus the ramp does not provide significantly better efficiencies with the 50 μm I.D. capillary in our case.

To investigate the influence of the capillary diameter on the peak widths with and without the initial voltage ramp, we

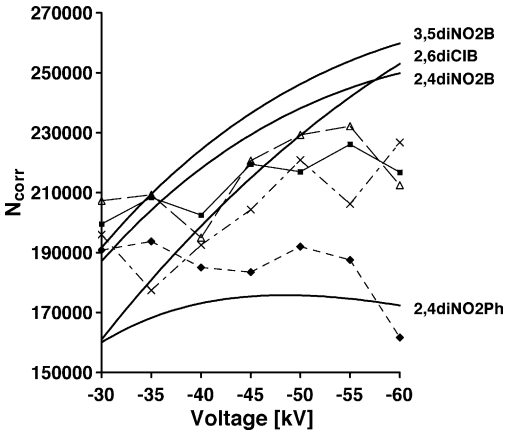

Fig. 3. Corrected plate numbers (symbols) obtained experimentally using 50 μm I.D. coated capillary with 30 s initial voltage ramp and calculated plate numbers (solid lines) at various separation voltages. For other parameters, see Figs. 1 and 2.

carried out additional runs in 100 and 75 μm I.D. capillaries. The results for the 100 μm I.D. capillaries are presented in Fig. 4 for 30 and 45 kV. As can be seen, the 30 s initial voltage ramp has a substantial reducing effect on the peak widths, especially at 45 kV, but the effect is fairly strong even at 30 kV. We note that we could not apply voltages above 45 kV with the 100 μm I.D. capillaries because above 45 kV the BGE solution tended to boil at the capillary inlet. With the 75 μm I.D. capillaries at 45 kV, the 30 s voltage ramp yielded about 8-15% narrower peaks relative to the case of no ramp (data not shown). This is less than the corresponding decrease of 35–50% with the 100 μm I.D. capillaries. These results demonstrate that the initial abrupt voltage application results in pronounced dispersion only when wide capillaries are used at high field strengths. In all three capillaries, the initial voltage ramp had less effect on peak areas than on peak width.

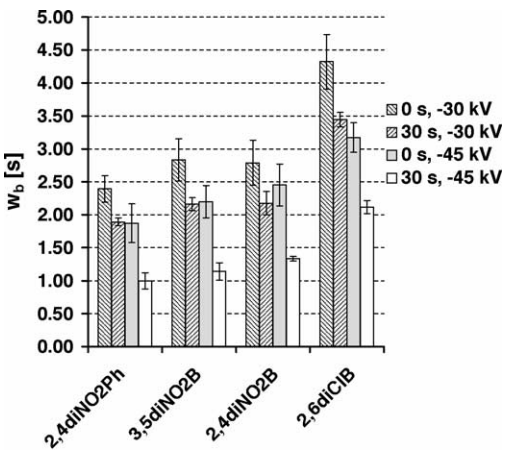

Fig. 4. Analyte peak widths obtained in 100 μm I.D. coated capillary using 15 mM acetate BGE with and without 30 s initial voltage ramp. Number of repetitions was 11. The height of the error bar is twice the standard deviation. For other parameters, see Fig. 1.

3.2. Influence of BGE ionic strength

To determine if heating effects were responsible for the lowered efficiency associated with the initial abrupt voltage application, the effect of ionic strength of the BGE solution on the peak widths was investigated by applying BGE solutions of different acetate concentrations, namely 5, 15 and 25 mM (acetic acid concentration is the same). The results obtained with two configurations: (i) 5 mM acetate solution with the 100 μm I.D. capillary and (ii) 25 mM acetate solution with the 50 μm I.D. capillary were compared with results obtained with the 15 mM acetate solution with a 100 μm or 50 μm I.D. capillary, respectively.

Reducing the acetate concentration from 15 to 5 mM (case i) should decrease the dispersion if heating effects are responsible for the additional dispersion observed with the 15 mM acetate solution in 75 and 100 μm I.D. capillaries. Indeed, the peak widths obtained at 30 kV with the 5 mM acetate BGE solution in 100 μm I.D. capillaries were approximately the same with and without the 30 s initial voltage ramp. At 45 kV, in turn, slightly narrower (5–17%) peaks were obtained with the 30 s voltage ramp than without the ramp. The difference was, however, not as large as with the 15 mM acetate BGE (Fig. 4). It is thus clear that decreasing the ionic strength of the BGE solution reduces the harmful influence of abrupt voltage application on the peak widths.

No additional dispersion relative to the no ramp conditions was observed with the 50 μm I.D. capillary at 15 mM (Section 3.1.4), and at 25 mM (case ii) the situation turned out to be very similar as can be seen in Fig. 5. Only slightly broader peaks were obtained at 60 kV when no ramp was used compared to the case of 30 s ramp. At 30 kV, however, the usage of the ramp did not offer any advantage. These observations (especially, case i) suggest that heating effects are responsible for the dispersion arising from the abrupt voltage application.

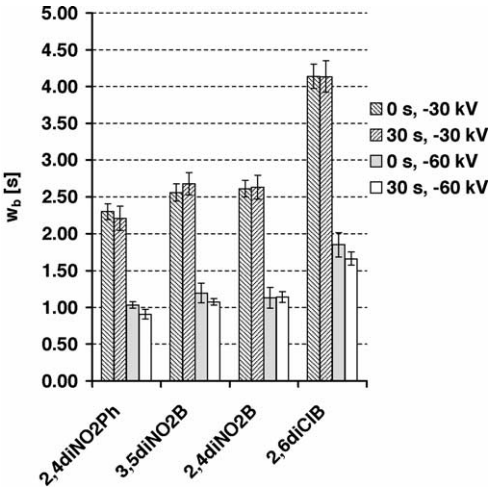

Fig. 5. Analyte peak widths obtained with 25 mM acetate BGE solution in 50 μm I.D. coated capillary with and without 30 s initial voltage ramp. For other parameters, see Figs. 1 and 4.

Table 1
Peak widths of 2,6-dichlorobenzoic acid, calculated heating powers and temperature differences and critical dU/dt values for various capillaries, voltages and BGE concentrations

Capillary I.D. (μm)	U (kV)	c (BGE) (mM)[a]	t_{ramp} (s)	w_b (2,6diCIB) (s)[b]	EI (W/m)	ΔT_{inlet} (°C)[c]	(dU/dt)$_{crit}$ (kV/s)[d]
50	30	15	0	3.34	0.6	4	9.2
50	30	15	30	3.27 (98%)	0.6	4	9.2
50	60	15	0	1.39	2.5	18	6.5
50	60	15	30	1.36 (98%)	2.5	18	6.5
50	30	25	0	4.14	0.7	5	7.5
50	30	25	30	4.14 (100%)	0.7	5	7.5
50	60	25	0	1.85	3.1	22	5.0
50	60	25	30	1.66 (90%)	3.1	22	5.0
75	30	15	0	3.21	1.1	8	4.3
75	30	15	30	3.28 (102%)	1.1	8	4.3
75	60	15	0	2.20	5.3	38	2.3
75	60	15	30	1.32 (60%)	5.3	38	2.3
100	30	15	0	4.32	3.2	23	1.2
100	30	15	30	3.44 (80%)	3.2	23	1.2
100	45	15	0	3.17	7.7	55	0.8
100	45	15	30	2.12 (67%)	7.7	55	0.8
100	30	5	0	2.35	0.9	6	5.8
100	30	5	30	2.52 (107%)	0.9	6	5.8
100	45	5	0	1.65	2.1	15	4.6
100	45	5	30	1.41 (85%)	2.1	15	4.6

[a] This value is for added concentration of NaAc; same amount of HAc was added.
[b] Values in parenthesis were calculated from w_b (30 s ramp)/w_b (0 s ramp) × 100%.
[c] $k_b = 0.174\,W\,m^{-1}\,K^{-1}$, $k_s = 1.380\,W\,m^{-1}\,K^{-1}$, $k_p = 0.155\,W\,m^{-1}\,K^{-1}$, $r_w = 172.5\,\mu m$, $r_p = 187.5\,\mu m$, $T_{ambien} = 23\,°C$, $h_1 = 130\,W\,m^{-1}\,K^{-1}$ [4,6].
[d] R_Ω was calculated from $E = R_\Omega I$ for each combination of BGE concentration, capillary I.D. and voltage. $\mu_{2,6diCIB} = -7.5 \times 10^{-9}\,m^2\,V^{-1}\,s^{-1}$ [19], $\alpha_{PT} = 12\,K\,m\,W^{-1}$ [16], $\delta = 0.023\,K^{-1}$, γ (25 °C) $= 1.09 \times 10^{-3}\,K^{-1}$ [28].

3.3. Heating power and voltage ramp

As shown above, the dispersion resulting from abrupt voltage application is very likely associated with thermal effects. It was of interest, therefore, to investigate the thermal conditions in the capillary further. Table 1 lists the calculated heating powers, temperature differences at the capillary inlet (compared with ambient temperature) and critical dU/dt values (Eq. (7)) for the various capillaries, voltages and BGE concentrations used in this study. Peak widths of 2,6-dichlorobenzoic acid are also listed. It can be seen that at EI above 2–3 W/m, the initial abrupt voltage application has a significant effect on the peak widths and thus on the corresponding separation efficiencies.

The calculated temperature differences listed in Table 1 are reasonable, especially when it is considered that, with the 100 μm I.D. capillary above 45 kV, boiling of the BGE solution (EtOH boils at 78.2 °C) was observed at the capillary inlet, and that the calculated temperature at the capillary inlet is about 78 °C at 45 kV (Table 1). The closeness of these two values also suggests that the value $130\,W\,m^{-2}\,K^{-1}$ [6,13] used for the inlet surface heat transfer coefficient is quite appropriate in our case. Note, however, that Eq. (8) tends to slightly overestimate the temperature difference because the field strength E_1 in the unthermostatted region is lower than the nominal field strength [U/(L_1+L_2+L_3)].

As noted in Section 3.1.1, separation efficiencies at 60 kV with the 75 μm I.D. capillary and 15 mM BGE concentration were best with the 30 s ramp up time. This corresponds to $2\,kV\,s^{-1}$ dU/dt, which is close to the calculated value of $2.3\,kV\,s^{-1}$ for critical dU/dt (Table 1). Note, however, that the critical dU/dt values were calculated on the assumption that no sample escapes from the capillary and are not exactly related to dispersion effects. The temperature dependency of γ in the case of EtOH is small (<9%; 10–60 °C) [22] and thus we used the γ value at 25 °C in calculating critical dU/dt and ignored the temperature dependency of γ, which resulted in slightly overestimated critical dU/dt values.

The critical dU/dt values (Table 1) calculated for low voltages or with the 50 μm I.D. capillaries would suggest that use of a voltage ramp of a few seconds is beneficial. Our experimental findings (Sections 3.1.2 and 3.2), in turn, indicate that the voltage ramp does not offer significantly better separation efficiencies under these conditions. Most of this discrepancy can probably be explained by two things: (i) a section about 1.5 cm long at the beginning of the capillary is immersed in the BGE solution, which provides better heat dissipation than still air and (ii) the temperature increase inside the capillary is time dependent [23–25]. Because of immersion in the BGE solution the local power–temperature coefficient in the first part of the capillary would in reality be smaller than was assumed, and this would increase the calculated critical dU/dt values. Likewise, the time dependency of the temperature increase inside the capillary would increase the critical dU/dt value because the time scale of the analyte acceleration is much faster (10^{-12} s [26]) than that of the

temperature increase (order of 1 s [24]). This means that analytes would advance a short distance in the capillary before the capillary temperature (and thus ΔT_{inlet}) reaches its maximum value. These considerations could also explain why 15 s ramp times ($dU/dt = 4$ kV/s) in the 75 μm I.D. capillary provided nearly as good separation efficiencies as 30 s ramp times (Fig. 1B)

There seems to be, however, slight correlation between the calculated critical dU/dt values and the experimentally obtained w_b values (Table 1), which suggests that thermal volume expansion could be the phenomenon underlying the dispersion related to the initial abrupt voltage application. Evidently, when it comes to separation efficiencies, Eq. (7) could give rough estimates of critical dU/dt values, which could help to evaluate if a voltage ramp is needed to avoid additional dispersion related to the abrupt voltage application. Note that even considerable high voltage variations (high dU/dt) have very little effect on the total band broadening during the separation [27] once analytes move beyond the vicinity of the capillary inlet.

When the temperature conditions and the capillary resistance are the same, the thermal volume expansion is more pronounced with non-aqueous than aqueous BGEs for analytes of identical overall mobility in the two solvent systems (Eq. (7)). The difference is for the most part due to about four times higher γ values of most organic solvents used in CE compared to the corresponding value of water (2.6×10^{-4} K^{-1} at 25 °C) [28]. The application of a sufficient initial voltage ramp is thus of particular importance when non-aqueous BGE solutions are used at high heating powers.

3.4. Axial temperature gradients

As noted in Section 3.1.3, with the 75 μm I.D. capillary the efficiencies obtained experimentally are slightly worse than those predicted with the theoretical plate height model. This deviation from theory can probably be attributed to approximations made in the calculations. Dispersion due to axial temperature gradients [12,13] was not, however, considered in the theoretical model used, which could also explain the deviation. To assess the importance of the contribution of axial temperature gradients to the total plate height we used Eq. (1) to calculate H_T. Table 2 shows the results for 2,4-dinitrophenol with 15 mM NaAc + 15 mM HAc BGE in EtOH at 60 kV. Note that constant heat transfer conditions in each region were assumed. Thus, neither the influence of capillary insertion to the BGE solution in regions 1 and 3 nor the influence of the plastic fittings at the interfaces of the different regions was considered. The value for the surface heat transfer coefficient in the thermostatted region ($h_2 = 500$ W m^{-2} K^{-1}) was calculated as described in [29] (measured air flow velocity 7.7 ms^{-1}). H_T is about 0.1 μm for 2,4-dinitrophenol (Table 2), and less than this for the other analytes. This means that the combined contribution of axial and radial temperature gradients to the total plate height is in our case less than 8% even at high field strengths. In addition,

Table 2
Calculated plate height[a] of 2,4-dinitrophenol induced by both axial and radial temperature gradients and the parameters needed for the calculation

I	L (cm)	T_w (°C)[b]	ΔT_c (°C)	κ (S m^{-1})[c]	E (V cm^{-1})	η (Pa s)	M (m^2 Pa^{-1} s^{-1})	μ_{eo} (m^2 V^{-1} s^{-1})	P (Pa)	t (s)	v_{pd} (ms^{-1})[d]	D (m^2 s^{-1})	H_T (μm)
1	5	58	2.0	0.0288	−1730	6.24E − 04	2.85E − 07	−6.44E − 10	−3.12	12.9	7.35E − 05	1.05E − 09	0.014
2	23	33	2.3	0.0240	−2082	9.29E − 04	1.92E − 07	−4.33E − 10	1.25	73.4	5.72E − 05	6.50E − 10	0.076
3	2	58	2.0	0.0288	−1730	6.24E − 04	2.85E − 07	−6.44E − 10	–	5.2	3.80E − 05	1.05E − 09	0.001
Total													0.091

[a] 15 mM NaAc + 15 mM HAc in EtOH, 75 μm I.D. capillary, $U = -60$ kV, $L_{tot} = 30$ cm, $L_{det} = 28.5$ cm, $B = 1630$ K [19], $h_1 = h_3 = 130$ W m^{-2} K^{-1} [13], $h_2 = 500$ W m^{-2} K^{-1}.
[b] T_w was calculated from Eq. (8) by ignoring the term describing the temperature drop ΔT_c in the capillary core (i.e. term $l/2k_b$ was set to zero) and using either h_1 or h_2.
[c] Conductivities at T_w were estimated from experimental data reported in [17].
[d] $\mu_{i,ep}$ was calculated using the Stokes equation, $\mu_{i,ep} = (ze_0/6\pi r_0\eta_i)$, to account for the temperature dependence of μ_{ep} and thus v_{pd}; $r_0 = 6.4 \times 10^{-10}$ m.

radial temperature gradients (the second term on the right in Eq. (2)) contribute to v_{pd} (and thus to H_T) more than axial temperature gradients under our experimental conditions. The effect of axial temperature gradients on the separation efficiencies in our case is thus much smaller than suggested in Ref. [12]. The reason for the previously observed discrepancy [19] of the measured and predicted values was instead mainly the abrupt voltage application as discussed in Section 3.1.3.

We incorporated the dispersion arising from the combined effect of the axial and radial temperature gradients (Eq. (1)) in our previous model [19] and recalculated the separation efficiencies for our analytes at different field strengths. The results were practically identical to the results shown in Fig. 2. The very low dispersion due to axial temperature gradients in our case is due to the suppressed EOF, which will not induce strong pressure gradients (Eqs. (5) and (6)) even though axial temperature gradients in the capillary are marked (Table 2). At conditions of high heat generation (high E, r_c, κ) and with the presence of strong EOF, H_T can be quite large if the capillary is unevenly thermostatted in axial direction [12]. At such conditions the contribution of H_T should be included in the plate height model used for improved accuracy of the predictions.

4. Concluding remarks

Initial abrupt voltage application may markedly increase the dispersion of the analyte zones and lower the separation efficiency. We have shown that the dispersion arising from initial abrupt voltage application increases with increasing: (i) rate of voltage increase, (ii) final separation voltage, (iii) capillary diameter and (iv) ionic strength of the BGE solution. These trends in dispersion resemble those of Joule heating, which did not, however, significantly contribute to the total plate height through radial temperature gradients [19]. Our results strongly suggest that the dispersive effect of abrupt voltage application is of thermal origin and may be related to the thermal volume expansion of the sample and BGE solutions [15]. With a sufficiently long initial voltage ramp, the dispersive effect of voltage application can be avoided. The plate numbers reported here are in good agreement with the theoretical values calculated from the plate height model. The deviation of the measured separation efficiencies from the predicted values at high field strengths that we previously observed [19] was mainly caused by the initial abrupt voltage application. To our knowledge, the deteriorating effect of abrupt voltage application on separations has been emphasized by only a few groups [15,30–33]. Perhaps more attention should be paid to this especially when dealing with obstinate separations or trying to achieve maximum separation efficiencies. The influences of initial abrupt voltage application or axial temperature gradients on the separation efficiency are not, however, very significant in the conditions normally applied in CE ($EI < 3$ W/m, $r_c = 50$ μm).

Acknowledgements

Financial support was provided by the Magnus Ehrnrooth Foundation (S.P.) and the Academy of Finland (M.-L.R. and S.P., project number 206296). The authors thank Professor Ernst Kenndler and Dr. Simo Porras for helpful discussions during the preparation of this paper.

References

[1] S. Hjertén, Chromatogr. Rev. 9 (1967) 122.
[2] R. Virtanen, Acta Polytech. Scand., Chem. Incl. Metall. Ser. 123 (1974) 1.
[3] J.H. Knox, Chromatographia 26 (1988) 329.
[4] E. Grushka, R.M. McCormick, J.J. Kirkland, Anal. Chem. 61 (1989) 241.
[5] J.H. Knox, I.H. Grant, Chromatographia 24 (1987) 135.
[6] S.P. Porras, E. Marziali, B. Gaš, E. Kenndler, Electrophoresis 24 (2003) 1553.
[7] G.O. Roberts, P.H. Rhodes, R.S. Snyder, J. Chromatogr. 480 (1989) 35.
[8] J.K. Towns, F.E. Regnier, Anal. Chem. 64 (1992) 2473.
[9] C.A. Keely, T.A.A.M. van de Goor, D. McManigill, Anal. Chem. 66 (1994) 4236.
[10] B. Potoček, B. Gaš, E. Kenndler, M. Štědrý, J. Chromatogr. A 709 (1995) 51.
[11] A.E. Herr, J.I. Molho, M.G. Santiago, M.G. Mungal, T.W. Kenny, M.G. Garguilo, Anal. Chem. 72 (2000) 1053.
[12] X. Xuan, D. Li, Electrophoresis 26 (2005) 166.
[13] B. Gaš, J. Chromatogr. 644 (1993) 161.
[14] X. Xuan, D. Sinton, D. Li, Int. J. Heat Mass Transfer 47 (2004) 3145.
[15] J.H. Knox, K.A. McCormack, Chromatographia 38 (1994) 279.
[16] J.H. Knox, K.A. McCormack, Chromatographia 38 (1994) 207.
[17] S. Palonen, M. Jussila, S.P. Porras, T. Hyötyläinen, M.-L. Riekkola, Electrophoresis 23 (2002) 393.
[18] S. Palonen, S.P. Porras, M. Jussila, M.-L. Riekkola, Electrophoresis 24 (2003) 1565.
[19] S. Palonen, M. Jussila, S.P. Porras, M.-L. Riekkola, Electrophoresis 25 (2004) 344.
[20] S. Palonen, M. Jussila, S.P. Porras, T. Hyötyläinen, M.-L. Riekkola, J. Chromatogr. A 916 (2001) 89.
[21] B.A. Williams, G. Vigh, Anal. Chem. 67 (1995) 3079.
[22] T.F. Sun, C.A. Ten Seldam, P.J. Kortbeek, N.J. Trappeniers, S.N. Biswas, Phys. Chem. Liq. 18 (1988) 107.
[23] M.S. Bello, P.G. Righetti, J. Chromatogr. 606 (1992) 103.
[24] E.V. Dose, G. Guiochon, J. Chromatogr. A 652 (1993) 263.
[25] K.-L.K. Liu, K.L. Davis, M.D. Morris, Anal. Chem. 66 (1994) 3744.
[26] J.C. Giddings, Unified Separation Science, Wiley, New York, 1991, p. 43.
[27] H.K. Jones, N.T. Nguyen, R.D. Smith, J. Chromatogr. 504 (1990) 1.
[28] Y. Marcus, The Properties of Solvents, Wiley, Chichester, 1998, p. 67.
[29] J.H. Knox, K.A. McCormack, Chromatographia 38 (1994) 215.
[30] B.F. Johnson, E.S. Nordman, International Patent WO01/07904 A1 (2001).
[31] J. Sowell, R. Parihar, G. Patonay, J. Chromatogr. B 752 (2001) 1.
[32] S.R. Bean, G.L. Lookhart, Cereal Chem. 78 (2001) 530.
[33] F. Foret, L. Křivánková, P. Boček, Capillary Zone Electrophoresis, VCH, Weinheim, 1993, p. 88.